Molecular mechanisms that control initiation and termination of physiological depolarization-evoked transmitter release

Yonatan M. Kupchik*, Grigory Rashkovan*, Lily Ohana*†, Tal Keren-Raifman‡, Nathan Dascal‡, Hanna Parnas*, and Itzchak Parnas*§

*Department of Neurobiology, Hebrew University, Jerusalem 91904, Israel; and ‡Department of Physiology and Pharmacology, Tel Aviv University, Tel Aviv 69978, Israel

Edited by Eric R. Kandel, Columbia University, New York, NY, and approved January 14, 2008 (received for review September 9, 2007)

Ca^{2+} is essential for physiological depolarization-evoked synchronous neurotransmitter release. But, whether Ca^{2+} influx or another factor controls release initiation is still under debate. The time course of ACh release is controlled by a presynaptic inhibitory G protein-coupled autoreceptor (GPCR), whose agonist-binding affinity is voltage-sensitive. However, the relevance of this property for release control is not known. To resolve this question, we used pertussis toxin (PTX), which uncouples GPCR from its $G_{i/o}$ and in turn reduces the affinity of GPCR toward its agonist. We show that PTX enhances ACh and glutamate release (in mice and crayfish, respectively) and, most importantly, alters the time course of release without affecting Ca^{2+} currents. These effects are not mediated by $G_{\beta\gamma}$ because its microinjection into the presynaptic terminal did not alter the time course of release. Also, PTX reduces the association of the GPCR with the exocytotic machinery, and this association is restored by the addition of agonist. We offer the following mechanism for control of initiation and termination of physiological depolarization-evoked transmitter release. At rest, release is under tonic block achieved by the transmitter-bound high-affinity presynaptic GPCR interacting with the exocytotic machinery. Upon depolarization, the GPCR uncouples from its G protein and consequently shifts to a low-affinity state toward the transmitter. The transmitter dissociates, the unbound GPCR detaches from the exocytotic machinery, and the tonic block is alleviated. The free machinery, together with Ca^{2+} that had already entered, initiates release. Release terminates when the reverse occurs upon repolarization.

G protein-coupled receptor | neurotransmitter release | pertussis toxin | presynaptic receptors

Ca^{2+} influx is essential for physiological depolarization-induced neurotransmitter (NT) release (1, 2). A broader, Ca^{2+} voltage, hypothesis suggests that two factors control release: Ca^{2+} and G protein-coupled receptors (GPCRs), whose agonist-binding affinity is voltage-dependent (3). The mechanism suggested for this control is as follows. (*i*) At resting potential and rest concentration (nMs) of transmitter, the release machinery (SNARE proteins and synaptotagmin) is under tonic block imposed by the transmitter-bound high-affinity (nMs) GPCR. (*ii*) Depolarization shifts the GPCR to a low-affinity state (μMs), resulting in rapid transmitter dissociation (it should be emphasized that at this stage release of NT did not occur yet, and the concentration of NT in the synapse is still in the nM range). (*iii*) The unbound GPCR detaches from the release machinery to relieve the tonic block. The free-release machinery together with Ca^{2+}, which had already entered, initiates release. (*iv*) Upon repolarization, release terminates because the receptor returns to its high-affinity state and the tonic block is reinstated.

Much of this suggested mechanism was supported experimentally (3–8) by using mainly the cholinergic neuromuscular junction (NMJ), where the M_2 muscarinic autoreceptor (M_2R) controls both slow feedback inhibition (9, 10) and fast ACh release (6–8). However, the relevance of this hypothesis for other NTs was not investigated. More importantly, the mechanism underlying the tonic block is not known even for the cholinergic synapse. It could be produced by $G_{\beta\gamma}$ because it inhibits release by interacting with proteins of the release machinery (11, 12). Alternatively, it could be achieved by a direct interaction of M_2R with voltage-dependent Ca^{2+} channels (13), or it could result from the transmitter-bound M_2R directly interacting with the release proteins (14, 15). Finally, it was not demonstrated experimentally that the voltage-dependent affinity of the GPCRs plays the role assigned to it in points (*ii*)–(*iv*) above. The affinity of GPCRs was universally shown to be high when coupled to the G protein and low when uncoupled (16, 17). Pertussis Toxin (PTX) uncouples the GPCRs from their $G_{i/o}$ (18, 19), hence reducing their affinity toward their agonists, as was indeed shown for M_2R (5). We therefore used PTX to test whether the affinity of the GPCR plays a crucial role in release control. We conducted our experiments on NMJ and not in CNS synapses often used to study release [e.g., the calyx-of-Held (20)] because in the former it is easier to detect single quanta to establish directly synaptic delay histograms. These conditions are necessary to measure with high resolution the effect of PTX on the time course of release (measured by synaptic delay histograms) and test whether or not the effect of PTX is voltage-dependent.

Our results confirm that presynaptic GPCRs control release kinetics primarily by interacting with the release proteins rather than by employing $G_{\beta\gamma}$ or affecting Ca^{2+} channels. Furthermore, this interaction is most likely governed by changes in the affinity of the GPCR to the NT. This mechanism is likely a general one because it operates both in ACh and in glutamate (Glu) NMJs.

Results

PTX Increases Spontaneous and Evoked ACh Release and Alters Its Time Course. M_2R controls the time course (21) of ACh release without affecting Ca^{2+} currents (6–8). To examine whether the voltage-dependent affinity of M_2R is relevant for release control, we checked for effects of PTX on various aspects of ACh release in the mouse NMJ. In wild-type (WT) mice, PTX increased

Author contributions: Y.M.K., H.P., and I.P. designed research; Y.M.K., G.R., L.O., and T.K.-R. performed research; N.D. contributed new reagents/analytic tools; Y.M.K., G.R., and L.O. analyzed data; and Y.M.K., H.P., and I.P. wrote the paper.

The authors declare no conflict of interest.

This article is a PNAS Direct Submission.

†Present address: Division of Genetics and Development, Toronto Western Research Institute, University Health Network, Toronto, ON, Canada M5T 2S8.

§To whom correspondence should be addressed. E-mail: parnas@huji.ac.il.

This article contains supporting information online at www.pnas.org/cgi/content/full/0708540105/DC1.

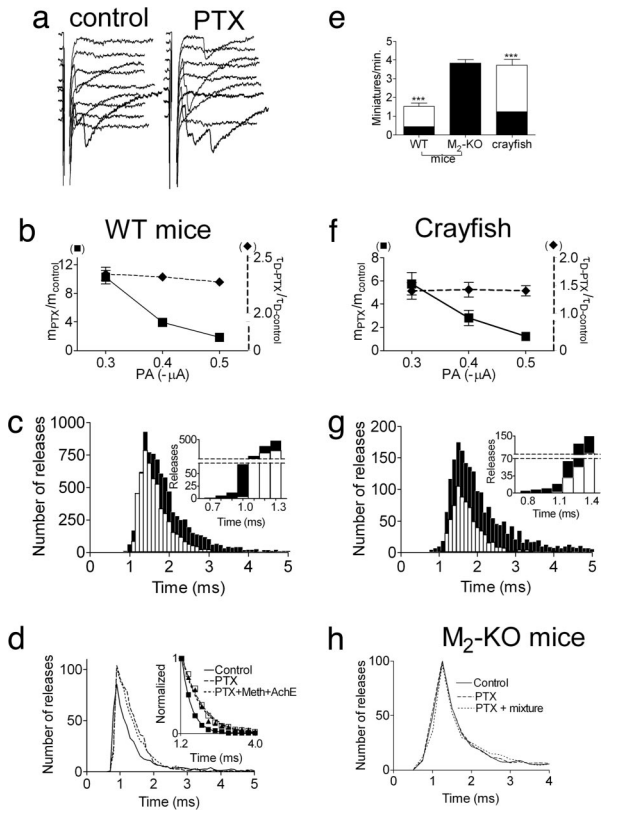

Fig. 1. Effect of PTX on ER and SR at the mouse and crayfish NMJ. Results are presented as mean ± SEM. *n*, number of muscles. (*a–d*) WT mice. (*a*) Sample traces of ER in controls and after PTX treatment. (*b*) PTX increased *m* in a voltage-dependent manner (■, *Left y* axis, $m_{PTX}/m_{control}$, $P < 0.0001$, $n = 5$) and τ_D in a voltage-independent manner (◆, *Right y* axis, $\tau_{D\text{-}PTX}/\tau_{D\text{-}control}$, $n = 4$). (*c*) Delay histograms recorded at −0.5 μA, 0.5 ms (total of 15,000 pulses, $n = 5$). PTX (filled bars) increased m from 0.39 (control, empty bars) to 0.61, prolonged τ_D from 0.34 ± 0.02 ms to 0.76 ± 0.09 ms, and shortened the minimal delay by 0.3 ms (*Inset*). (*d*) PTX (solid line) increased *m* from 0.14 ± 0.01 to 0.20 ± 0.03 and prolonged τ_D from 0.35 ± 0.01 ms to 0.78 ± 0.05 ms. Subsequent addition of 10 μM methoctramine + 50 μg/ml AChE (dotted line) did not further increase *m* (0.19 ± 0.03) or τ_D (*Inset*, 0.71 ± 0.06 ms) ($n = 3$). (*e*) PTX increased SR rate in WT mice (from 0.43 ± 0.01 to 1.52 ± 0.2 min^{-1}) and in crayfish (from 1.24 ± 0.4 to 3.71 ± 0.3 min^{-1}) but not in M_2-KO mice (3.83 ± 0.4 and 3.82 ± 0.3 min^{-1}). (*f* and *g*) Crayfish. (*f*) PTX increased m in a voltage-dependent manner (■, *Left y* axis, $m_{PTX}/m_{control}$, $P = 0.003$, $n = 4$) and τ_D in a voltage-independent manner (◆, *Right y* axis, $\tau_{D\text{-}PTX}/\tau_{D\text{-}control}$, $n = 3$). (*g*) Delay histograms recorded at −0.35 μA, 0.6 ms (15,000 pulses). PTX (filled bars) increased *m* from 0.075 in control (empty bars) to 0.216, increased τ_D from 0.54 ± 0.04 ms to 0.87 ± 0.1 ms, and shortened the minimal delay by 0.3 ms (*Inset*). (*h*) M_2-KO mice (5,000 pulses, $n = 3$ for each condition). *m* and τ_D were 0.19 ± 0.04 and 0.41 ± 0.02 ms in control (solid line) and remained 0.2 ± 0.02 and 0.40 ± 0.04 ms with PTX. Subsequent addition of the mixture (dotted line) did not change *m* (0.19 ± 0.03) or τ_D (0.35 ± 0.04 ms).

spontaneous release (SR) ≈3-fold (Fig. 1*e*) but had no effect on the single quantum event [supporting information (SI) Figs. 7 and 8*a*], confirming a presynaptic effect of PTX (22).

The effect of PTX on evoked release (ER) (samples in Fig. 1*a*) was more complex. It increased the quantal content (*m*) at low depolarization (−0.3 μA, $m_{PTX}/m_{control} = 10.3 \pm 0.9$) with a smaller effect at higher depolarizations (−0.5 μA, $m_{PTX}/m_{control} = 1.9 \pm 0.1$) (Fig. 1*b*). PTX also affected release kinetics: release started 300 μs earlier (30% acceleration) (Fig. 1*c*, *Inset*, and SI Fig. 8*b*) and lasted longer: the time constant of decay (τ_D) increased from 0.34 ± 0.02 ms to 0.76 ± 0.09 ms (Fig. 1 *c* and *d* and SI Fig. 8*c*). This effect is also detected in a cumulative plot of the delays (SI Fig. 8*d*). The increase in τ_D after PTX treatment was independent of pulse amplitude (PA) (Fig. 1*b*; ≈2.3-fold on average).

PTX increased SR rate (3.62-fold) and *m*, in a voltage-dependent manner (6.7-fold at −0.3 μA; 1.44-fold at −0.5 μA) also at 37°C (mouse physiological temperature; data not shown). However, PTX effects on the time course of release could not be measured at this temperature because of its extreme brevity.

PTX Slows Reinstatement of the M_2R-Imposed Tonic Block. The results in Fig. 1 suggest that a PTX-sensitive GPCR is involved in control of initiation and termination of ACh release. We first examined whether the effects of PTX are mediated by M_2R by using NMJs of knockout mice lacking functional M_2R (M_2-KO) (23). Here, PTX had no effect on SR (Fig. 1*e*) or ER (Fig. 1*h*).

We then investigated the mechanism that underlies release termination. Termination of ACh release was slower when binding of ACh to the M_2R was retarded (3). Retardation was achieved either by the addition of methoctramine, a specific antagonist of M_2/M_4 GPCRs, or by reducing the ACh concentration in the synaptic cleft by the addition of ACh esterase (AChE) (7). If PTX prolongs release by retarding ACh binding, it should occlude the effect of methoctramine + AChE (mixture, coapplied to maximize retardation). This was indeed the case. In control, *m* was 0.14 ± 0.01 and τ_D was 0.35 ± 0.01 ms. After PTX treatment, they were increased to 0.20 ± 0.03 ($P < 0.0001$) and 0.78 ± 0.05 ms, respectively ($P < 0.0001$; Fig. 1*d*). Subsequent addition of the mixture did not further increase or prolong release; *m* and τ_D were 0.19 ± 0.03 and 0.71 ± 0.06 ms, respectively (Fig. 1*d*). Similarly, after exposure to the mixture, a subsequent incubation with PTX had no further effect (data not shown). In M_2-KO mice, the addition of PTX together with the mixture had no effect on ER (Fig. 1*h*).

These results suggest that PTX prolongs ACh release by permanently lowering the affinity of the GPCR, consequently retarding the rebinding of ACh to M_2R upon membrane repolarization and neutralizing the reinstatement of the M_2R-imposed tonic block. Under such conditions, we expect that removal of Ca^{2+} will determine release termination (3). Indeed, although in PTX-untreated mice the addition of the Ca^{2+} chelator 1,2-bis(2-aminophenoxy)ethane-*N*,*N*,*N*′,*N*′-tetraacetic acid tetrakis(acetoxymethyl ester) (BAPTA-AM) did not shorten release kinetics (3, 8), in PTX-treated mice it did shorten release (SI Fig. 9).

PTX Increases Glu SR and ER and Alters Its Time Course. Presynaptic GPCRs have not been shown to control initiation and termination of Glu release. The crayfish NMJ, which has many similarities to mammalian CNS synapses (24), is convenient to study release of Glu (25, 26). Several studies demonstrated the presence of metabotropic glutamatergic receptors in crustaceans (27–30). Also, unpublished observations (Y.M.K., H.P., and I.P., unpublished results) indicate that, in the crayfish NMJ, the control of the time course of Glu release is achieved by a metabotropic Glu receptor (mGluR) of the group II type. We therefore checked for effects of PTX on release in crayfish NMJ. Indeed, the effects of PTX on Glu release are similar to those seen for ACh release in WT mice (Fig. 1 *f* and *g* and SI Fig. 8 *e–h*).

PTX Does Not Affect Ca^{2+} Currents. Because GPCRs inhibit Ca^{2+} channels in a voltage-dependent manner (13, 31–34), PTX could potentially enhance ER by abolishing this block. We measured presynaptic Ca^{2+} currents derived from the excitatory nerve terminal current (ENTC) (7, 8, 35). Because PTX does not enhance release at high depolarizations (Fig. 1 *b* and *f*), the amplitude of the action potential had been reduced (see *Materials and Methods*). Fig. 2 shows that both in mouse (Fig. 2*a*) and crayfish (Fig. 2*c*), PTX increased ER produced by the smaller action potential. Yet, the amplitude and kinetics of the Ca^{2+} current (Fig. 2 *b* and *d*) did not change. That this technique is

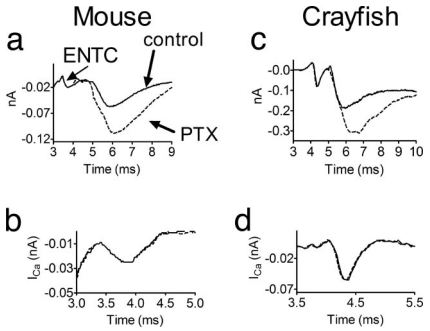

Fig. 2. PTX increased the synaptic currents without affecting the Ca^{2+} currents. (*a* and *b*) WT mice. (*a*) PTX (broken line) increased the synaptic current without affecting the ENTC. (*b*) Ca^{2+} currents (superposition) were the same before and after PTX treatment. (*c* and *d*) Same as in *a* and *b*, but in crayfish.

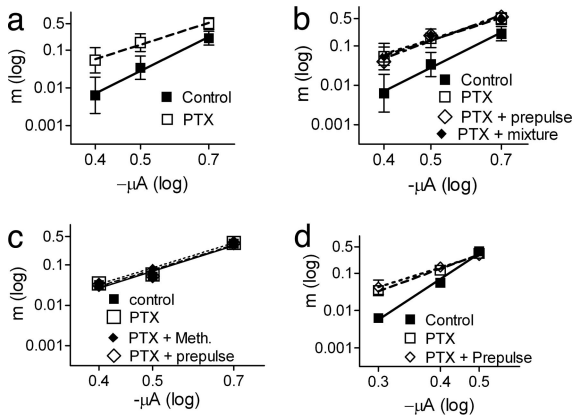

Fig. 3. PTX affects the {log *m*/log (PA)} slope. (*a* and *b*) WT mice. (*a*) Control slope, 6.18 ± 1.93 (■). After PTX, 3.95 ± 1.41 (□, $n = 5$, $P < 0.0001$). (*b*) Control slope, 7.48 ± 0.96 (■). After PTX (□, 3.95 ± 1.41), subsequent addition of the mixture (♦) or a depolarizing prepulse (◇, −1.0 μA, 0.1 ms, preceding the test pulse by 1 ms) did not further reduce the slope (3.96 ± 1.2 or 4.10 ± 0.34, respectively) ($n = 5$). (*c*) M_2-KO mice. Control slope, 4.33 ± 0.36 (■) and 4.21 ± 0.39 after PTX (□). Subsequent addition of 10 μM methoctramine (♦) or administration of a prepulse (◇) did not affect the slope (4.21 ± 0.39, 4.33 ± 0.35, respectively) ($n = 3$). (*d*) Crayfish. PTX (□) reduced the slope from 7.03 ± 0.39 in control (■) to 3.92 ± 0.45. Administration of a prepulse (−1.0 μA, 0.1 ms, preceding the test pulse by 1 ms) after PTX (◇) did not further reduce the slope (3.37 ± 0.58).

able to detect changes in Ca^{2+} currents had they occurred is evident from comparing Ca^{2+} currents produced by full- and reduced-size action potentials (SI Fig. 10 *a* and *c*) or at two $[Mg^{2+}]_o$ (SI Fig. 10 *b* and *d*).

PTX Relieves the Tonic Block of ACh and Glu Release. What then is the mechanism involved in release initiation? In ACh release, depolarization plays a dual role: (*i*) opening Ca^{2+} channels (fast) and (*ii*) relief of the ACh-bound M_2R-imposed tonic block (slightly slower) (3, 6). To reveal the latter, the nerve terminal was depolarized to different levels at fixed $[Ca^{2+}]_o$, and the relationship between *m* and the amplitude of the depolarizing pulse (PA) (expressed as the slope of [log *m*/log PA]) was measured under control conditions and when the M_2R-imposed tonic block was eliminated by addition of an antagonist or by administration of a strong but very brief depolarizing prepulse (see *SI Methods*) preceding test pulses of variable amplitudes (6). In both cases, the slope of [log *m*/log PA] was reduced, suggesting that under physiological conditions depolarization plays the two roles. If so, then the slower of the two, relief of the tonic block, governs release initiation. Only when the tonic block does not exist does depolarization fulfill the first role alone, opening Ca^{2+} channels (6).

We repeated these experiments with and without PTX. In PTX-treated WT mice, *m* increased in a voltage-dependent manner: from 0.006 ± 0.002 to 0.05 ± 0.03 (8.3-fold) at −0.4 μA but only from 0.21 ± 0.07 to 0.50 ± 0.15 (2.4-fold) at −0.7 μA. Consequently, the [log *m*/log PA] slope declined from a control value of 6.18 ± 1.93 to 3.95 ± 1.41 ($P < 0.0001$; Fig. 3*a*). Addition of the mixture or administration of the depolarizing prepulse after PTX treatment had no further effect on the slope (Fig. 3*b*). These results suggest that PTX too relieves the tonic block imposed by M_2R, presumably by shifting M_2R into low affinity toward ACh (5, 16, 17).

Not surprisingly, PTX had no effect on the slope in M_2-KO mice. The control slope was lower to begin with (4.33 ± 0.36); after PTX treatment it was 4.21 ± 0.39, and it remained so after subsequent manipulations (Fig. 3*c*).

Similarly to WT mice, in crayfish, PTX increased release in a voltage-dependent manner, and the effect of the prepulse was occluded with PTX pretreatment (Fig. 3*d*).

Muscarine and Glu Reverse the Effect of PTX. If PTX indeed prolongs release by reducing the affinity of the GPCRs toward their agonists, then a higher concentration of the agonists is expected to reverse release prolongation. This expectation was met for both WT mice (SI Fig. 11*a*) and crayfish (SI Fig. 11 *b* and *c*) NMJs.

The Tonic Block of Release Is Not Mediated by $G_\beta\gamma$. Although the results so far are compatible with the hypothesis that PTX exerts its effect on release by reducing the affinity of GPCRs toward their agonist, another explanation should be considered. $G_\beta\gamma$ was shown to inhibit transmitter release (11, 12) without affecting Ca^{2+} currents. It is thus possible that PTX exerts its effects by reducing the levels of $G_\beta\gamma$.

Microinjection of $G_\beta\gamma$ into the crayfish axon preterminal reduced *m* by ≈70% with a recovery time (that presumably reflects diffusion away of the $G_\beta\gamma$) of ≈10 min ($m_{control} = 0.13 \pm 0.02$ and $m_{G\beta\gamma} = 0.04 \pm 0.01$; Fig. 4*a*, a representative experiment). This inhibition was not accompanied by changes in the time course of release (Fig. 4*b*); the minimal delay and τ_D remained the same as in control (Fig. 4*b Inset*). As shown in ref. 12, $G_\beta\gamma$ did not affect Ca^{2+} currents (Fig. 4*f*). Microinjection of denatured $G_\beta\gamma$ did not reduce *m* (SI Fig. 12*a*).

We next microinjected $G_\beta\gamma$ into PTX-treated terminals. Here too, $G_\beta\gamma$ inhibited release by ≈65% (similar to its effect without PTX treatment) (Fig. 4*c*) but did not reverse the effects on τ_D ($\tau_D = 0.70 \pm 0.03$ with PTX, and $\tau_D = 0.71 \pm 0.02$ after injecting $G_\beta\gamma$; Fig. 4*d*). Together, these results show that the effects of PTX are not caused by reduction of the $G_\beta\gamma$ concentration.

Reinforcement of this conclusion is provided in Fig. 4*e*. Although PTX enhanced release in a voltage-dependent manner (Fig. 1 *b* and *f*), the magnitude of $G_\beta\gamma$ inhibition was independent of pulse amplitudes; it was 44.9 ± 2.6% at −0.5 μA and 45.3 ± 4.1% at −0.9 μA ($P > 0.9$; for raw data see SI Fig. 12*b*). This finding, together with the lack of effect of $G_\beta\gamma$ on the time course of release, suggests that the physiological tonic inhibition that is relieved by depolarization is not mediated by $G_\beta\gamma$. It is presumably also not mediated by G_α because injection of guanosine 5′-(3-*O*-thio)triphosphate ($GTP_\gamma S$) inhibited release in a voltage-independent manner and did not affect the time course of release (SI Fig. 13).

PTX Reduces the Physical Interaction Between M_2R and Syntaxin. The results so far are compatible with the notion that under physiological conditions the tonic block is achieved by a direct association of the transmitter-bound high-affinity receptor with the release pro-

NEUROSCIENCE

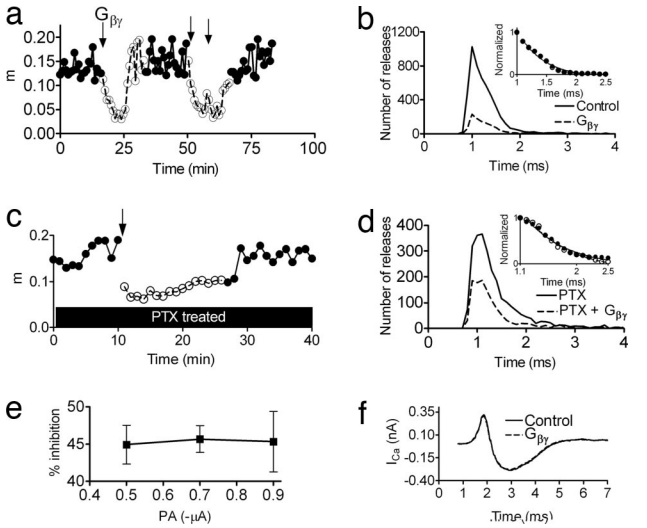

Fig. 4. $G_{\beta\gamma}$ inhibits release in a voltage-independent manner without altering the time course of release at the crayfish NMJ at 12 ± 1°C. Pulses are 5 Hz. $[G_{\beta\gamma}]_{electrode}$, 4 μM. (*a*) Representative experiment. Similar results were obtained in three more experiments. $G_{\beta\gamma}$ microinjection (first arrow) lowered *m* from 0.13 ± 0.02 in control (●) to 0.04 ± 0.01 (○). Its effect lasted for ≈10 min. Two consecutive injections (arrows) of $G_{\beta\gamma}$ (10-min interval) reduced release for ≈20 min. (*b*) Total of 30,000 pulses, $n = 4$. $G_{\beta\gamma}$ lowered *m* from 0.12 ± 0.03 in control (solid line) to 0.03 ± 0.01 (broken line) but did not change τ_D (*Inset*, 0.34 ± 0.04 ms in control and 0.33 ± 0.04 ms with $G_{\beta\gamma}$) or the minimal delay (0.6 ms in control and with $G_{\beta\gamma}$). (*c*) $G_{\beta\gamma}$ microinjection to a PTX-treated terminal lowered *m* from a maximum of 0.19 to a minimum of 0.068 (64% inhibition) (a representative experiment is shown; similar results were obtained in two more experiments). (*d*) Total of 15,000 pulses, $n = 3$. First, PTX alone was applied [solid line, $m = 0.16 \pm 0.01$, $\tau_D = 0.70 \pm 0.03$ (*Inset*)]. Subsequent $G_{\beta\gamma}$ microinjection (broken line) reduced *m* to 0.07 ± 0.01 but did not affect τ_D (*Inset*, $\tau_D = 0.71 \pm 0.02$). (e) $G_{\beta\gamma}$-induced inhibition is voltage-independent. It was 44.9 ± 2.6% at PA of −0.5 μA, 45.7 ± 1.8% at −0.7 μA, and 45.3 ± 4.1% at −0.9 μA ($n = 4$). (*f*) Injection of $G_{\beta\gamma}$ did not affect Ca^{2+} currents (solid line, control; broken line, $G_{\beta\gamma}$).

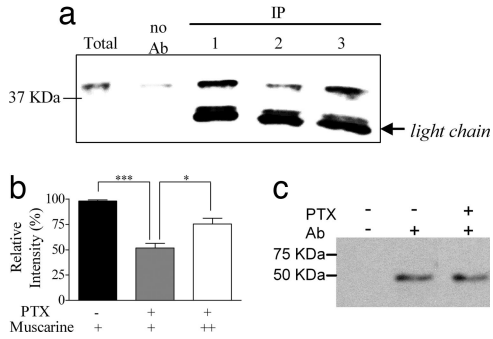

Fig. 5. PTX affects the interaction between M_2R and syntaxin. IP experiments were performed by using mAb against M_2R. (*a*) A representative immunoblot detected with mAb against syntaxin. Immunoreactivity of the Ab used in the IP experiment is marked as light chain. Lanes: 1, control, with 100 nM muscarine; 2, PTX with 100 nM muscarine; 3, PTX, with 20 μM muscarine. Initial amount of syntaxin was the same under all treatments. (*b*) Average relative immunoreactivity of syntaxin from four experiments similar to that described in *a*, presented as percentage of control. The SEM of the control was calculated from duplicates. Black bar, control. Gray and white bars, PTX with 100 nM (+) and 20 μM (++) muscarine, respectively. *, $P = 0.011$; ***, $P < 0.0001$. (*c*) Representative immunoblot detected with (+) or without (minus) mAb against M_2R, in the presence (+) or absence (minus) of PTX.

teins (3). A further test of the above conclusion would be to measure the effect of PTX on the coimmunoprecipitation (IP) of the M_2R and the release proteins. Because PTX reduces the affinity of M_2R toward its agonist (4, 5), it is expected also to diminish the interaction of the M_2R with the release proteins. Furthermore, a subsequent addition of a high concentration of the agonist is expected to restore this interaction.

IP experiments were conducted with fresh mouse brain synaptosomes (pretreated with AChE to hydrolyze endogenous ACh). Co-IP of M_2R with one representative of the SNARE proteins, syntaxin, was examined. It is seen (Fig. 5*a*, compare *Upper* lanes 1 and 2) that PTX reduced the co-IP of M_2R with syntaxin. On average, PTX treatment reduced the M_2R–syntaxin interaction to 52 ± 4% of control (Fig. 5*b*; $P < 0.0001$) but did not affect the amount of precipitated M_2R (Fig. 5*c*). Addition of 20 μM muscarine restored most of the M_2R–syntaxin interaction (to 75 ± 6% of the control, $P = 0.01$) (Fig. 5*a*, lane 3, and Fig. 5*b*).

Discussion

The primacy of Ca^{2+} in physiological depolarization-induced synchronous release is amply documented (1, 2, 21, 36). Surprisingly, the time course of physiological release was found to be independent of Ca^{2+} level and kinetics (37–39) [in contrast to Ca^{2+}-uncaging-induced release (2, 40), where release kinetics heavily depends on Ca^{2+} level], suggesting that another factor, somewhat slower in its effect than Ca^{2+} entry, limits triggering of depolarization-evoked release. In several studies we have shown that this factor is a presynaptic GPCR, whose agonist-binding affinity is voltage-dependent (6–8). The present work, although not aimed at elucidating the role of Ca^{2+} in release, enables nevertheless a clear discrimination between release aspects controlled by Ca^{2+} and those controlled by GPCRs. The negligible effect of PTX on the amount of release at high depolarizations implies that this feature of physiological release is determined predominantly by Ca^{2+}. However, the lack of effect of PTX on the level and kinetics of Ca^{2+} currents together with its salient effect on release kinetics suggests that the latter is controlled by the GPCR. With this dual control of depolarization and Ca^{2+}, the amount of NT release can be modulated during repetitive stimulation while keeping the time course of release unaltered, a property that is critical for information processing (3).

Fig. 6 illustrates our suggested mechanism for GPCRs + Ca^{2+}-mediated control of release. In the present work, using PTX, we substantiated our assumption that it is the voltage-dependent agonist-binding affinity of the GPCRs that is crucial for formation and relief of the tonic block. Because of the rapidity of release (a few milliseconds), it is unlikely that second messengers are involved in control of the tonic block. Rapid control could potentially be achieved (*i*) by GPCRs targeting Ca^{2+} channels (31, 34, 41), (*ii*) by GPCRs targeting the release machinery via $G_{\beta\gamma}$ (11, 12, 42), or (*iii*) by a rapid voltage-dependent shift of the GPCR affinity and a direct interaction of the GPCR itself with the release machinery (14, 15).

Several lines of evidence render possibilities (*i*) and (*ii*) unlikely. We showed here that PTX affects release without altering Ca^{2+} currents. Also, the voltage dependence of GPCR-mediated inhibition of the Ca^{2+} channels is achieved because depolarization causes dissociation of $G_{\beta\gamma}$ from the channels (18, 43, 44). However, we have shown here that the inhibition of release by $G_{\beta\gamma}$ is voltage-independent. Moreover, inhibition of NT release by $G_{\beta\gamma}$ does not alter Ca^{2+} entry (Fig. 4*f* and ref. 12). This result, together with our observation that $G_{\beta\gamma}$ did not affect the time course of Glu release (Fig. 4), implies that the possibility that $G_{\beta\gamma}$ mediates the tonic block by interacting either with Ca^{2+} channels (*i*) or directly with SNARE proteins (*ii*) is unlikely.

Our results are best explained by possibility (*iii*), i.e., rapid control of ER is achieved by GPCRs shifting their affinity toward their NT in a voltage-dependent manner. The affinity shift affects binding of the GPCR to the NT, which in turn affects the

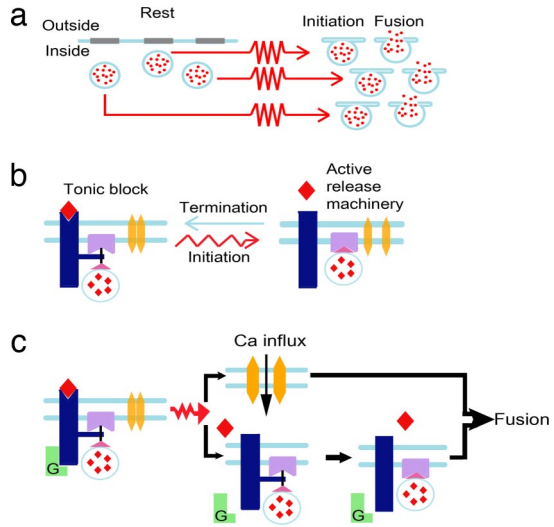

Fig. 6. Schematic representation of the mechanism suggested for control of initiation and termination of physiological depolarization-induced NT release. The processes are described at three levels of resolution. (*a*) Lowest resolution. At resting potential, the vesicles [blue circles with NT (red dots)] are ready for release, but release does not commence. After the arrival of the action potential (red arrows), changes in the release machinery occur (initiation), which enable fusion. Several vesicles will be able to undergo initiation and fusion before termination commences. (*b*) Low level resolution of the initiation and termination processes. At resting potential, the high-affinity NT (red rhombus)-bound GPCR (dark blue) interacts directly with the release proteins (purple), imposing tonic block of release. The Ca^{2+} channel (yellow) is closed. Upon depolarization, Ca^{2+} channels open, and, independently, the GPCR shifts to a low-affinity state. The NT dissociates, the unbound GPCR detaches from the release proteins, the tonic block is alleviated, and release initiates. Upon membrane repolarization (blue arrow), the tonic block is reinstated. (*c*) High-level resolution of release initiation, focusing on the different kinetics of Ca^{2+} influx and tonic block alleviation. Upon the arrival of the action potential, two independent events occur quickly on a very similar time scale (indicated by the two processes presented one below the other): influx of Ca^{2+} and, independently, the G protein detaches from the GPCR, shifting it to a low-affinity state, so that the NT dissociates. Then, with a bit slower rate, the unbound GPCR detaches from the release proteins. The free-release machinery, together with the Ca^{2+} that had already entered, enables fusion of the vesicle with the cell membrane.

direct interaction between the GPCR and the release machinery. In this framework, PTX affects initiation and termination of release by shifting the GPCR to a low-affinity state toward the transmitter; termination of release will be slower because of retardation of the rebinding of the NT, thus delaying reinstatement of the block. Initiation occurs sooner because at rest, only a small fraction of the PTX-mediated low-affinity receptor will be bound to the agonist present in the synaptic cleft, resulting in more "free" release machinery to be encountered by the rapid influx of Ca^{2+}. Also, the voltage-dependent enhancement of release after PTX treatment (Figs. 1 and 3) can be explained in this framework because a strong test pulse (i.e., high depolarization) by itself is sufficient to remove most of the tonic block, so PTX becomes redundant.

We presented results indicating that voltage-sensitive presynaptic GPCRs are involved in the control of transmitter release by interacting directly with the release proteins (rather than with Ca^{2+} channels). This interaction adds to already known direct couplings of GPCRs with various effectors (45; for review, see ref. 46). We show, however, that the coupling of the GPCR to the release proteins is both voltage- and agonist-dependent. Hence, interaction of GPCRs with other proteins might also be under dual control of agonist and membrane potential.

In conclusion, in this work we investigated physiological depolarization-induced synchronous release from NMJs. We believe that the same mechanisms apply for synchronous release in the CNS because the basic release properties of NMJ and CNS are similar (see for example, ref. 24). Further studies are necessary to determine whether the mechanisms described here are also relevant for other modes of release, e.g., Ca^{2+}-triggered release (2), asynchronous release, and release induced by hypertonic solutions (47, 48).

Materials and Methods

See *SI Methods* for a more detailed description.

Animals. ***Mice.*** Mice were 1.5–3 months old. The Sabra line of white mice was used unless stated otherwise. M_2-KO mice [mixed genetic background (129JIXCF; 50%/50%) (23)] and age-matched WT mice were kindly provided by Jürgen Wess (Laboratory of Bioorganic Chemistry, National Institute of Diabetes and Digestive and Kidney Diseases, received from Taconic Farms) were used. Results obtained in the Sabra mice resembled those of the control WT mice. Mice were anesthetized with CO_2 and decapitated according to institutional guidelines and the Israeli law for animal protection. For electrophysiology, hemidiaphragm neuromuscular preparations were isolated and submerged in the standard bathing solution (15 ± 1°C) as described in ref. 8. Here and in crayfish, small changes in Ca^{2+} and Mg^{2+} concentration (1–3 mM) were not compensated for, TTX was added only in focal depolarization, and pH was adjusted to 7.4 with NaOH.

Crayfish. The L1 bundle of the deep extensor abdominal muscles or the opener muscle of the first two walking legs of 4–8-cm-long (head-to-tail) *Procambarus clarkii* crayfish (Shalom Hayat Biological Preparatory) were exposed and submerged in a modified Van Harreveled solution (10 ± 1°C, unless otherwise stated) as described before (49, 50).

Electrophysiology. Macropatch electrode was used for stimulation and recording as described before (mice, refs. 6 and 8; crayfish, refs. 26 and 50). Briefly, the terminal was stimulated with focal depolarizing pulses of 0.5–0.6 ms and amplitude varying between −0.3 and −0.9 μA at a rate of 1–5 Hz. Single quanta were easily discerned (Fig. 1*a*). *m* is obtained directly by dividing the number of quanta released within 10 ms after every pulse by the number of applied pulses. The rate of SR (no stimulation) was determined for a period of 30 min before and after PTX treatment and was very low (less than 4 min^{-1} in both preparations). Hence, there is no need to take it into account in the evaluation of *m*. For synaptic delay histograms (21), the delay to each quantum was measured. Delays were grouped into bins of 0.1 or 0.25 ms. Connecting the bin mid points gave a continuous delay histogram. At least 5,000 pulses were given for histogram reliability. The number of pulses was the same in controls and after the different experimental treatments (see *SI Methods*).

Exposure to Drugs and PTX Treatment. The preparation was immersed in a constantly circulating solution (Minipuls 3 peristaltic pump; Gilson). Drugs were added to the reservoir beaker. For PTX incubation, fluid circulation was stopped and temperature increased to 25 ± 1°C. PTX was added directly to the recording chamber (1 μg/ml). After 2–3 h the pump was reactivated, and recording was resumed. Two to three hours of incubation was shown to be sufficient for PTX activation (51) and for reducing muscarine-mediated autoinhibition of ACh release (10). Here, it diminished Glu-induced inhibition (SI Fig. 7*a*). Heat-inactivated (80°C for 30 min) PTX had no effect on release (SI Fig. 7*b*).

PTX, methoctramine, muscarine, and L-glutamic acid (monosodium salt) were purchased from Sigma. TTX was from Alomone Labs. AChE was kindly provided by Israel Silman (Weizmann Institute, Rehovot, Israel) or purchased from Sigma.

$G_{\beta\gamma}$ Microinjection. $G_{\beta\gamma}$ (purified recombinant $G_{\beta1\gamma2}$) was kindly provided by Carmen W. Dessauer (University of Texas, Houston) and stored as described (52, 53) in a stock solution (40 μM). Denatured $G_{\beta\gamma}$ was obtained by heating to 70°C for 10 min. It was pressure-injected (54) (pico-injector PLI-100; Medical Systems) into the opener excitor axon preterminal of the crayfish by using a back-filled microelectrode and the Burleigh controller 6000 stepper (Burleigh Instruments). The first daughter branch of the axon was impaled distally to the main bifurcation ≈50 μm from the recording site. The electrode solution consisted of 4 μM $G_{\beta\gamma}$, 150 mM KCl, 10 mM Tris buffer, and 0.4% dextrane–rhodamine B (Molecular Probes); the pH was adjusted to 7.2 with KOH.

Ca^{2+} Current Measurements. Ca^{2+} currents were measured as described (7, 8, 35). To assure that the PTX affects *m*, the action potential was reduced either by adding 50 nM TTX and 10 mM triethanolamine to the bathing solution (in the mouse experiments) or by reducing $[Na^+]_o$ to 55 mM (in crayfish experiments) as described (55).

Immunoprecipitation. IP experiments and detection of the precipitated proteins were done as described (14, 15). The Abs used for Western blot analyses were monoclonal anti-syntaxin (1:10,000; Transduction Laboratories) and monoclonal anti-M_2R (1:500; Alomone Labs) (see *SI Methods*).

Statistical Analysis. Data are presented as average ± SEM. τ_D is presented as best fit ± error of fit. Significance was obtained with Student's two-tailed paired or unpaired *t* test in all figures. All statistical analyses were performed by using GraphPad Prism version 4.03 for Windows (GraphPad Software).

ACKNOWLEDGMENTS. We are grateful to Dr. Wess for the M_2-KO mice, Dr. Silman for the AChE, and Dr. Dessauer for the $G_{\beta 1\gamma 2}$. We are grateful to Dr. D. Parnas for reading of the manuscript and many useful comments. Special thanks to the Goldie-Anna Fund and Dr. Kenneth Stein (New York) for continuous support.

1. Augustine GJ (2001) *Curr Opin Neurobiol* 11:320–326.
2. Schneggenburger R, Neher E (2005) *Curr Opin Neurobiol* 15:266–274.
3. Parnas H, Parnas I (2007) *Trends Neurosci* 30:54–61.
4. Ben-Chaim Y, Chanda B, Dascal N, Bezanilla F, Parnas I, Parnas H (2006) *Nature* 444:106–109.
5. Ben-Chaim Y, Tour O, Dascal N, Parnas I, Parnas H (2003) *J Biol Chem* 278:22482–22491.
6. Parnas H, Slutsky I, Rashkovan G, Silman I, Wess J, Parnas I (2005) *J Neurophysiol* 93:3257–3269.
7. Slutsky I, Silman I, Parnas I, Parnas H (2001) *J Physiol (London)* 536:717–725.
8. Slutsky I, Wess J, Gomeza J, Dudel J, Parnas I, Parnas H (2003) *J Neurophysiol* 89:1954–1967.
9. Slutsky I, Parnas H, Parnas I (1999) *J Physiol (London)* 514:769–782.
10. Slutsky I, Rashkovan G, Parnas H, Parnas I (2002) *J Neurosci* 22:3426–3433.
11. Blackmer T, Larsen EC, Bartleson C, Kowalchyk JA, Yoon EJ, Preininger AM, Alford S, Hamm HE, Martin TF (2005) *Nat Neurosci* 8:421–425.
12. Blackmer T, Larsen EC, Takahashi M, Martin TF, Alford S, Hamm HE (2001) *Science* 292:293–297.
13. Hamilton BR, Smith DO (1991) *J Physiol (London)* 432:327–341.
14. Ilouz N, Branski L, Parnis J, Parnas H, Linial M (1999) *J Biol Chem* 274:29519–29528.
15. Linial M, Ilouz N, Parnas H (1997) *J Physiol (London)* 504:251–258.
16. Gilman AG (1987) *Annu Rev Biochem* 56:615–649.
17. Kenakin T (1997) *Trends Pharmacol Sci* 18:456–464.
18. Tedford HW, Zamponi GW (2006) *Pharmacol Rev* 58:837–862.
19. Fields TA, Casey PJ (1997) *Biochem J* 321:561–571.
20. Schneggenburger R, Forsythe ID (2006) *Cell Tissue Res* 326:311–337.
21. Katz B, Miledi R (1965) *Proc R Soc London Ser B* 161:483–495.
22. Sugiura Y, Ko CP (2000) *Neuroreport* 11:3017–3021.
23. Gomeza J, Shannon H, Kostenis E, Felder C, Zhang L, Brodkin J, Grinberg A, Sheng H, Wess J (1999) *Proc Natl Acad Sci USA* 96:1692–1697.
24. Atwood HL, Cooper RL (1996) *J Neurosci Methods* 69:51–58.
25. Dudel J (1981) *Pflügers Arch* 391:35–40.
26. Ravin R, Parnas H, Spira ME, Volfovsky N, Parnas I (1999) *J Neurophysiol* 81:634–642.
27. Parnas I, Dudel J, Parnas H, Ravin R (1996) *Eur J Neurosci* 8:116–126.
28. Krenz WD, Nguyen D, Perez-Acevedo NL, Selverston AI (2000) *J Neurophysiol* 83:1188–1201.
29. Le Ray D, Cattaert D (1999) *J Neurosci* 19:1473–1483.
30. Perez-Acevedo NL, Krenz WD (2005) *Brain Res* 1062:1–8.
31. Dolphin AC (2006) *Br J Pharmacol* 147 (Suppl 1):S56–S62.
32. Patil PG, de Leon M, Reed RR, Dubel S, Snutch TP, Yue DT (1996) *Biophys J* 71:2509–2521.
33. Takago H, Nakamura Y, Takahashi T (2005) *Proc Natl Acad Sci USA* 102:7368–7373.
34. Zamponi GW, Snutch TP (1998) *Curr Opin Neurobiol* 8:351–356.
35. Dudel J (1990) *Pflügers Arch* 415:566–574.
36. Parnas H, Segel L, Dudel J, Parnas I (2000) *Trends Neurosci* 23:60–68.
37. Andreu R, Barrett EF (1980) *J Physiol (London)* 308:79–97.
38. Datyner NB, Gage PW (1980) *J Physiol (London)* 303:299–314.
39. Hochner B, Parnas H, Parnas I (1991) *Neurosci Lett* 125:215–218.
40. Bollmann JH, Sakmann B (2005) *Nat Neurosci* 8:426–434.
41. Hille B (1994) *Trends Neurosci* 17:531–536.
42. Gerachshenko T, Blackmer T, Yoon EJ, Bartleson C, Hamm HE, Alford S (2005) *Nat Neurosci* 8:597–605.
43. Bean BP (1989) *Nature* 340:153–156.
44. Kasai H, Aosaki T (1989) *Pflügers Arch* 414:145–149.
45. Lohse MJ, Benovic JL, Codina J, Caron MG, Lefkowitz RJ (1990) *Science* 248:1547–1550.
46. Bockaert J, Fagni L, Dumuis A, Marin P (2004) *Pharmacol Ther* 103:203–221.
47. Sudhof TC (2004) *Annu Rev Neurosci* 27:509–547.
48. Sun J, Pang ZP, Qin D, Fahim AT, Adachi R, Sudhof TC (2007) *Nature* 450:676–682.
49. Parnas I, Atwood HL (1966) *Comp Biochem Physiol* 18:701–723.
50. Ravin R, Spira ME, Parnas H, Parnas I (1997) *J Physiol (London)* 501:251–262.
51. Rathmayer W, Djokaj S (2000) *J Comp Physiol A* 186:287–298.
52. Kozasa T (1999) *G Proteins*: *Techniques of Analysis*, ed Manning DR (CRC Press, Boca Raton, FL), pp 23–37.
53. Peleg S, Varon D, Ivanina T, Dessauer CW, Dascal N (2002) *Neuron* 33:87–99.
54. Parnas I, Rashkovan G, O'Connor V, El-Far O, Betz H, Parnas H (2006) *J Neurophysiol* 96:1053–1060.
55. Parnas I, Parnas H, Dudel J (1982) *Pflügers Arch* 393:232–236.